Colloids and Surfaces B: Biointerfaces 145 (2016) 688–694

Contents lists available at ScienceDirect

Colloids and Surfaces B: Biointerfaces

journal homepage: www.elsevier.com/locate/colsurfb

Distinctive colonization of *Bacillus* sp. bacteria and the influence of the bacterial biofilm on electrochemical behaviors of aluminum coatings

Leila Abdoli, Xinkun Suo, Hua Li*

Key Laboratory of Marine Materials and Related Technologies, Key Laboratory of Marine Materials and Protective Technologies of Zhejiang Province, Ningbo Institute of Materials Technology and Engineering, Chinese Academy of Sciences, Ningbo 315201, China

ARTICLE INFO

Article history:
Received 2 February 2016
Received in revised form 15 May 2016
Accepted 26 May 2016
Available online 27 May 2016

Keywords:
Microbial corrosion
Biofilm
Aluminum
Microscopy
Bacteria
Electrochemical testing

ABSTRACT

Formation of biofilm is usually essential for the development of biofouling and crucially impacts the corrosion of marine structures. Here we report the attachment behaviors of *Bacillus* sp. bacteria and subsequent formation of bacterial biofilm on stainless steel and thermal sprayed aluminum coatings in artificial seawater. The colonized bacteria accelerate the corrosion of the steel plates, and markedly enhance the anti-corrosion performances of the Al coatings in early growth stage of the bacterial biofilm. After 7 days incubation, the biofilm formed on the steel is heterogeneous while exhibits homogeneous feature on the Al coating. Atomic force microscopy examination discloses inception of formation of local pitting on steel plates associated with significantly roughened surface. Electrochemical testing suggests that the impact of the bacterial biofilm on the corrosion behaviors of marine structures is not decided by the biofilm alone, it is instead attributed to synergistic influence by both the biofilm and physicochemical characteristics of the substratum materials.

1. Introduction

It has been well established that biofouling occurred in early stage involves predominately formation of a biofilm on substratum materials [1]. For controlling biofouling in the marine environment, it is essential to understand the development of biofilm and its influence on anti-corrosion performances of marine structures. Biofilm usually reduces the exposure of solid surfaces to external environment by forming a protective layer on the surfaces. However, in most cases, biofilm could result in local corrosion and consequently deteriorated performances of substratum materials [2–4]. Microorganisms within the biofilms formed on the surfaces of metallic materials could influence kinetics of cathodic and/or anodic reactions [5] and change electrochemical conditions at metal/solution interfaces, leading to either accelerated or inhibited corrosion [6,7]. The presence of microorganisms on a metal surface often gives rise to formation of corrosive oxygen concentration cell, alternation of electrolyte ion concentration or bacteria-induced inactivation of corrosion inhibitor [8]. These microorganisms and their metabolic activities have been reported to influence severely the corrosion process by stimulating localized corrosion, depending on the formation of passive film and the surface modification capabilities of metals [9,10]. Clarification of colonization behaviors of typical marine bacteria on marine structures and their effect on evolvement of bacteria-related biofilm might be the key for developing antifouling techniques.

Surface properties, e.g. chemistry, roughness, etc., of marine structures certainly affect the bacteria attachment. It was found that under identical environmental conditions, *Bacillus mycoides* accelerated the corrosion of zinc plates or coatings, decreased the corrosion rate of aluminum, and showed no effect on the corrosion behaviors of mild steel [11]. Alnnasouri et al. [12] investigated the effect of surface roughness on the long-term development of biofilms and realized that surface irregularities introduced on biofilm bed improved adhesion of the biofilm. Researchers have observed greater cell attachment on rougher surfaces and thus claimed surface roughness as an important factor in regulating bacterial attachment to inert surfaces [13,14]. It is usually believed that initial colonization of bacteria starts from surface irregularities such as cracks, pores, or abrasion defects, and subsequently spreads out from these areas [15–17]. Initial adhesion preferably starts at the locations where bacteria are sheltered against shear forces. Under flow conditions, hydrodynamic shear forces are important factors to affect biofilm development by altering mass transport, substrate access or detachment probability. When the shear force is higher, biofilm would detach from the surface more easily. In the case of rougher surfaces, biofilm is usually trapped in the grooves and is protected effectively from shear forces. The changes from reversible

* Corresponding author.
E-mail address: lihua@nimte.ac.cn (H. Li).

http://dx.doi.org/10.1016/j.colsurfb.2016.05.075
0927-7765/

to irreversible attachment can be established more easily in these sites. Moreover, roughening of the surface increases the areas available for bacterial adhesion. Other variables for instance the features of biofilm and chemistry of the substratum materials must also be considered.

Stainless steels are usually susceptible to localized corrosion in chloride-containing media, for instance offshore atmosphere and seawater, regardless of their widespread use for marine infrastructures. Microbiological activity plays an important role in pitting corrosion of stainless steel in the marine environment [18,19]. As a typical surface modification technique, thermal spray has been proven to be effective for protecting marine structures against corrosion through providing inorganic layers for maintenance-free long-term services. The technique offers the advantages of cost-efficiency, wide selection of coating materials and easy on-site operation [20–24]. Among thermal sprayed marine coatings, aluminum coatings performed well in the marine environment [25,26], predominately due to the fact that aluminum can act as sacrificial anode in the environment with high chloride contamination. However, there are so far few reports available focusing on biocorrosion behaviors of thermal sprayed marine coatings. In this work, stainless steel 316L and arc sprayed Al coatings were employed as typical marine materials for investigating colonization behaviors of *Bacillus* sp. on their surfaces. Biocorrosion mechanisms were examined and elucidated by microstructural characterization, electrochemical assessment, and simulation of the liquid/metal interfaces.

2. Materials and methods

For Al coating deposition, stainless steel 316L plates with a dimension of 20 × 20 × 2 mm were used as substrates. The coatings were deposited using a high velocity arc spray system (AS, TLAS-500C, China). The current and voltage of the arc were 100 A and 25 V, respectively. The spray distance was 150 mm. Compressed air with a pressure of 0.5 MPa was used as the auxiliary gas. Prior to the spraying, the substrates were degreased ultrasonically in acetone followed by grit blasting using 60 mesh black fused alumina sand.

Microstructure of the coatings was characterized by field emission scanning electron microscopy (FESEM, FEI Quanta FEG 250, the Netherlands). Biofilms formed on the surfaces of the SS plates were further analyzed by atomic force microscopy (AFM, 3100 SPM, Digital Instrument, USA) operated in air with the tapping mode (RTESP tip cantilever, spring constant: 40 N/m). To remove biofilm and clarify its effect on the substratum, pickling was done by immersing the coupons in an ultrasonic bath for 5 min in water and subsequent 2 min in 17% HNO_3 solution. For the corrosion testing of the coatings, potentiodynamic polarization and electrochemical impedance spectroscopy (EIS) spectra were acquired using a Solartron Modulab system (2100A, UK). All tests were conducted at room temperature in artificial seawater (ASW) prepared according to the ASTM D1141-98 (2003). Peptone with a concentration of 3 g/L was added into the media as carbon and energy sources for the bacteria. The media were adjusted to pH 7 and autoclaved at 121 °C for 20 min. Before the electrochemical measurement, the coating samples were immersed in ASW contained in an aerobic chamber under sterile conditions and in the presence of bacteria. The samples were then incubated at 30 °C in a shaker at 120 rpm. Each set of experiments was repeated three times to ensure reproducibility. A traditional three-electrode cell was used, with 1 cm^2 platinum as the counter electrode, a saturated calomel electrode (SCE) as the reference electrode and the specimen with an exposure area of 1 cm^2 as the working electrode. The surfaces were also sterilized with UV illumination and 70% ethanol for 1 h. EIS measurement was performed with an applied ac signal of 10 mV and the frequency ranging from 100 kHz to 0.01 Hz. After the measurement, the acquired data were fitted and analyzed using a ZSimpWin software based on equivalent circuit models. The equivalent circuits were chosen based on the number of time constants and quality of the fits [27,28]. Potentiodynamic polarization curves were acquired with a potential range from −500 mV to 500 mV vs E_{ocp} at a scan rate of 0.5 mVs^{-1}.

Bacillus sp. bacteria (MCCC1A00791, Marine Culture Collection of China) were chosen for the microbially influenced corrosion (MIC) testing. The medium for culturing *Bacillus* sp. was prepared by dissolving 1 g yeast extract and 5 g peptone in 1000 mL ASW. The media containing the bacterial strains were shaken for 24 h at 30 °C. Bacterial number was determined based on the standard calibration with an assumption that an OD_{600nm} value of 1.0 is equivalent to 10^9 bacteria/mL. The inoculated medium was prepared by adding *Bacillus* sp. for an initial concentration of 10^6 bacteria/ml at 30 °C under an aerobic condition. The biofilm formed on the surfaces of the coatings was characterized by Fourier transformed infrared spectroscopy (FTIR, Nicolet 6700, Thermo Fisher Scientific, USA) with the resolution of 4 cm^{-1} and a scan range of 4000–400 cm^{-1}.

3. Results and discussion

The arc sprayed Al coatings show dense structure with rough surface morphology (Fig. S1 in the Supplemental Data). Phase analyses already suggested undetected phase changes of Al during the coating fabrication (Fig. S1 in the Supplemental Data). To investigate the biofilm formation and its effect on MIC, the SS 316L plates and the Al coating samples were immersed in the ASW solutions with/without the bacteria for 7 and 30 days, respectively. It is noted that the SS 316L plates incubated in the bacteria-free ASW remained almost intact after 7 and 30 days exposure in the inoculated solution. Only a few corrosion attacks are visible on their surfaces, which is likely due to the presence of chloride ions (Fig. 1a). For the SS 316L plates immersed in the bacteria-containing ASW, colonization of *Bacillus* Sp. bacteria on their surfaces are clearly seen (Fig. 1b). It is apparent that a biofilm layer covers the surface. However, it is noted that after removal of the biofilm by cleaning with acid solution, small shallow pits are seen on the surface (Fig. 1c), suggesting pitting corrosion as a result of colonization of the bacteria.

For the Al coatings, it is noted that after 7 days incubation in the bacteria-free ASW solution, no marked changes are seen on their surfaces (data not shown), but after 30 days, damaged oxide layer is realized (Fig. 1d). For the coatings immersed in the bacteria-containing ASW, colonization of the bacteria on the coatings can be seen clearly (Fig. 1e). Bacterial adhesion initially occurs at the areas with flaws, e.g. microsized pores and cracks, on the surfaces of the coatings. Subsequent accumulation and further growth of the bacteria are seen around these areas. Development of a biofilm is usually facilitated by production of extracellular polymeric substances (EPS) [29], which comprise the macromolecules like proteins, polysaccharides, nucleic acids and lipids, and promotes adhesion of bacteria to biofilm matrix [30]. The capability of EPS to bind metal ions is important to MIC [31–33] and depends on bacterial species and the type of metal ions [34]. Metal binding by EPS involves the interaction between metal ions and anionic functional groups (e.g. carboxyl, phosphate, sulfate, glycerate, pyruvate and succinate groups). In addition, it is noted that the biofilm grown on the coating surface becomes homogeneous as the immersion time is prolonged (Fig. 1e,f). In the case of 7 days immersion, the surface of the coatings is also restrained naked even though the bacteria have interconnected with each other in some areas in particular those close to the pores (Fig. 1e). 30 days immersion of the

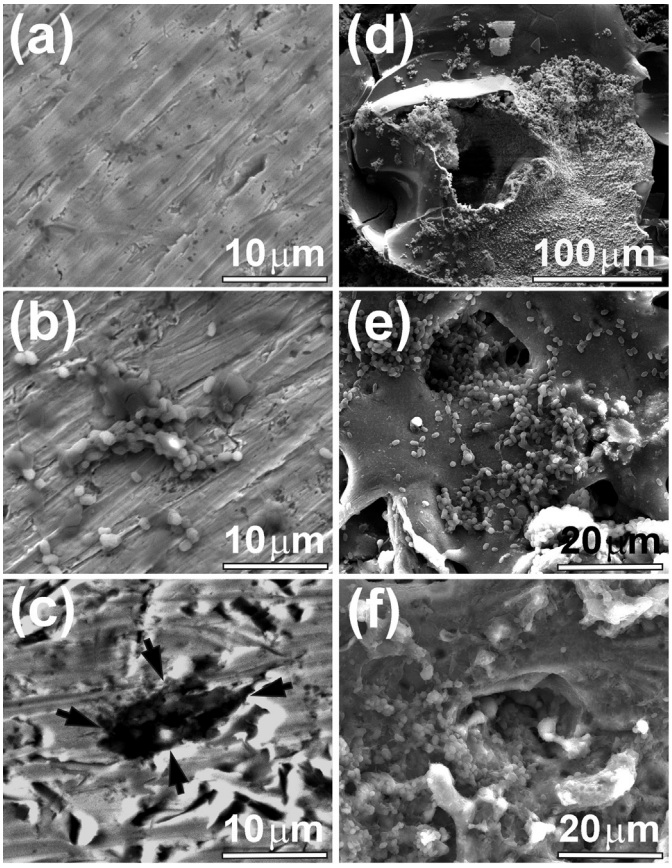

Fig. 1. FESEM images of the samples after being soaked in the ASW with/without *Bacillus* sp. bacteria. (a) the steel sample after 30 days incubation in the bacteria-free ASW showing almost non changes on its surface, (b) the steel sample shows clear colonization of the bacteria after 30 days soaking the bacteria-containing ASW, and (c) after the removal of the bacteria, the steel sample shows clear pitting on its surface (the arrows point to typical pitting area); (d) the Al coating after 30 days immersion in the bacteria-free ASW showing damaged surface, (e) after 7 days incubation in the bacteria-containing ASW, the Al coating shows remarkable colonization of the bacteria, and (f) a homogeneous bacterial biofilm has completely covered the surface of the Al coating after 30 days incubation.

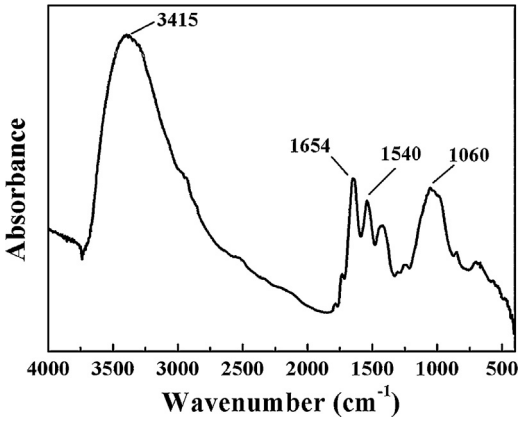

Fig. 2. FTIR spectrum of the bacterial biofilm formed on the surfaces of the samples.

samples already gives rise to full coverage of the coating surface by a homogeneous biofilm (Fig. 1f).

There is so far limited information available about the bacteria-related biofilm. Further characterization of the biofilm by FT-IR detection reveals a strong absorption peak at ~3415 cm^{-1} for stretching vibrations of O—H (the functional group in polysaccharides and proteins) and ~1060 cm^{-1} for —CO— stretching (glycopeptides, ribose) (Fig. 2). The IR band located at 1654 cm^{-1} refers to C=O and C—N (Amide I) stretching, and the peak at 1540 cm^{-1} reflects combination of NH bending and C—N (Amide II) stretching (Amide I and Amide II refer to the functional groups in proteins) [35,36]. These structural features of the biofilm further suggest that EPS of the bacteria colonized on the surfaces of the coatings taking part in the formation of the biofilm.

Among the surface properties of marine materials, surface roughness is believed to be an important factor affecting the formation and characteristics of biofilm [37]. Rough surface usually favors bacterial attachment [38], which probably accounts in part for the formation of more homogeneous biofilm on the surfaces of the Al coating than on the SS 316L plates. As a supplementary test to study the effect of surface roughness on the bacteria adhesion, thermal sprayed SS 316L coatings were also prepared and tested in inoculated medium. SEM images show consistent results that on the SS 316L plates with smooth surface, bacteria attachment is sparse while thicker films formed on rougher surfaces of the SS 316L coatings after 7 days incubation (Fig. S2 in the Supplemental Data). This further evidences the phenomena that rough surface facilitates attachment and colonization of the bacteria.

Further AFM observation of the surfaces of the SS 316L plates immersed in ASW for 30 days in absence or presence of the bacteria show remarkably different topographical morphology (Fig. 3). AFM has been widely recognized to be of higher resolution and accuracy in the vertical dimension than other microscopic techniques, hence offers an opportunity to characterize localized corrosion [39,40]. It is found that in absence of the bacteria, the SS 316L plates exhibit a relatively smooth and pit-free surface morphology (Fig. 3a). After immersion in the bacteria-containing ASW, ready colonization of the bacteria is clearly shown (Fig. 3b). After removal of the bacterial biofilm, obvious damage is seen on the surface area that was covered by the biofilm (Fig. 3c). These suggest biofilm-triggered corrosion. Furthermore, AFM observation shows that during the corrosion process, surface roughness of the SS 316L increases significantly in the bacteria-containing solution in comparison with the sterile condition. Local pitting is developed on the 316L surface in addition to general corrosion. Our ongoing efforts are devoted to further clarifying the effect of colonization of the bacteria on occurring of local pitting of the surface.

Effect of the biofilm on electrochemical corrosion behaviors of the steel plates and the coatings was further investigated. EIS assessment is able to provide clear insight into corrosion reaction mechanisms [41]. Typical Nyquist and Bode plots acquired for the samples immersed in the sterile ASW and the ASW with *Bacillus* sp. are shown in Fig. 4 and Fig. S3. The Bode plots were added to represent the impedance spectra since the magnitude of impedance at low frequencies is several orders higher than those at high frequencies. Thus, high-frequency features are difficult to discern in a Nyquist plot. The increased impedance value of the steel samples is presumably due to formation of oxide and corrosion product layers on the metal surface. However, in the bacteria-containing solution, the impedance value decreased significantly after 7 days exposure. This might be explained by diminished protective effects. The increased impedance value after 30 days incubation might result from the presence of the biofilm on the metal surface, which offers a passivation effect. That might also be due to possible surface modification of the metal stemming from metal oxidation triggered by the bacteria [42]. However, this layer is not homogeneous and could yield the corrosive conditions required by chloride ions that penetrate into the inner parts of the passive layer or biofilm [43]. In addition, under aerobic conditions, microbial colonization usually leads to the production of differential aeration and concentration cells because of the metabolism of the bacterial colony. Generation

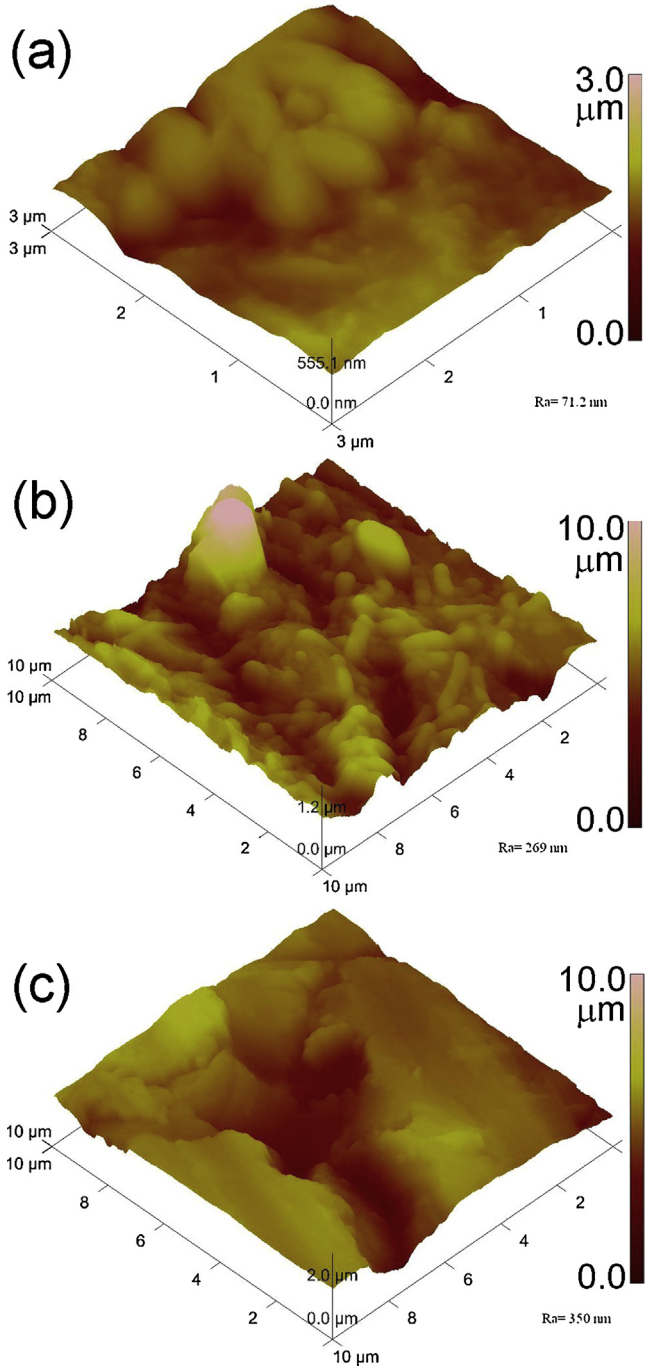

Fig. 3. AFM topographical images of the stainless steel plates after incubation for 30 days in the ASW without (a) and with (b) the bacteria, (c) demonstrates the obvious pitting of the steel after the removal of the bacterial biofilm shown in (b).

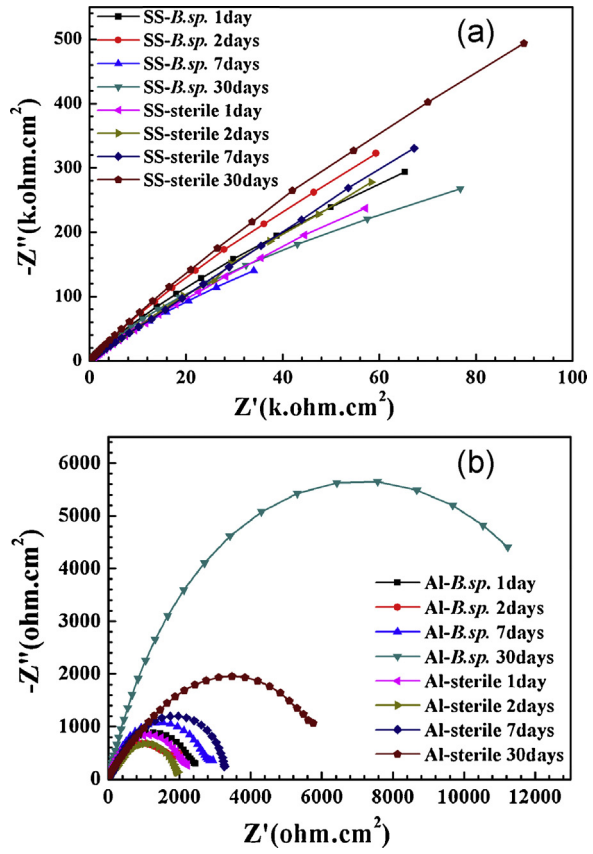

Fig. 4. Nyquist plots for the stainless steel plates (a) and the Al coatings (b) incubated in the ASW without (-sterile) or with (-*B.*sp.) the bacteria. SS: SS 316L plates, Al: aluminum coatings.

of these concentration cells is detrimental to the integrity of passive film [44] and enhances susceptibility of stainless steel to corrosion.

To illustrate the impedance response of the corrosion phenomena in the sterile ASW and the bacteria-containing ASW, equivalent circuits are proposed (Fig. 5a). In the equivalent circuit models, the contribution of various phenomena, such as electrical double layer, passive film, biofilm formation, laminar coating structure and others, are all taken into account. Only in the first and the second day, the steel coupons in the ASW with/without the bacteria fit the one-time constant model, R(QR), as illustrated in Fig. 5a-1. After incubation for 7 days and 30 days, the coupons in the bacteria-free ASW fit the two-time constant model, R(QR)(QR), as shown in Fig. 5a-2. $R_{ct}Q_{dl}$ describes the electrode Faraday process (corrosion process) and corresponds to the low-frequency impedance, while the circuit $R_{pf}Q_{pf}$ represents the formation of passive film on the metal surface and corresponds to the high-frequency impedance. The electric double layer exists at the interface between electrode and surrounding electrolyte. A three-time constant model was used to fit the experimental data in the bacteria-containing ASW after 7 and 30 days of exposure. Besides the passive film and the double layer, there appears to be a layer of porous biofilm on the steel surface (Fig. 5a-3). The model, R(Q(R(QR)(QR))), fits the experimental data favorably well. The fitted results are summarized in Table 1, and goodness of the fitting process can be deduced from the parameter of chi-square (χ^2). Obviously presence of the bacteria accelerates the corrosion of the stainless steel plates.

EIS measurements also suggest positive effect of the bacteria-associated biofilm on corrosion resistance of the coatings (Fig. 4b). It is realized that one month incubation already resulted in formation of homogeneous biofilm on the surfaces of the coatings. The biofilm significantly enhances the impedance of the coatings. The electrochemical impedance value increases as incubation time of the coating samples in the solution is prolonged, predominantly due to the formation of passive layer on the coating surfaces. Bacterial adhesion to a surface is a complicated process, which is affected by various physicochemical properties of both bacterial cells and substratum surfaces [45]. SEM characterization already disclosed that the bacterial adhesion occurred near the flaws on the surfaces of the coatings (Fig. 1e), from where biofilm started to form. The Nyquist spectra for the coatings in two testing media show two time constants (Fig. 4b). Based on the current EIS results as well as the electrochemical studies reported by Szczygiel et al. [46] on alumina-based composite coatings, an EIS equivalent circuit for the

Table 1
Electrochemical impedance parameters obtained from the best fitting of the experimental impedance diagrams of the surface/electrolyte interface determined by using ZSimpWin program (resistance amount is expressed as means ± SD from three independent experiments).

Sample	Rs (Ω cm^2)	R_{ct} (kΩ cm^2)	R_{pf} (Ω cm^2)	R_b (Ω cm^2)	CPE_{CT} (μF cm^{-2})	CPE_{pf} (μF cm^{-2})	CPE_b (μF cm^{-2})	$\chi^2(\times10^{-3})$
SS 316L								
in sterile ASW								
After 1 day	10.51	3887 ± 1.89	–	–	46.68	–	–	1.34
After 2 days	11.33	5261 ± 1.66	–	–	40.97	–	–	1.89
After 7 days	10.18	3733 ± 0.82	26.43 ± 0.02		34.21	74.72	–	2.98
After 30 days	11.53	6908 ± 0.74	13.13 ± 0.05	–	25.03	49.66	–	0.094
in ASW with bacteria								
After 1 day	10.37	4633 ± 1.20	–	–	42.06	–	–	1.66
After 2 days	10.45	4966 ± 0.64	–	–	38.74	–	–	0.411
After 7 days	10.7	1246 ± 1.53	48.06 ± 0.02	11.24 ± 0.04	85.91	85.02	71.09	0.035
After 30 days	13.37	2195 ± 0.84	5.224 ± 0.003	15.61 ± 0.21	150.6	43.27	44.05	0.093

Sample	R_s (Ω cm2)	R_{ct} (Ω cm2)	R_{coat} (Ω cm2)	R_b (Ω cm2)	CPE_{CT} (μF cm-2)	CPE_{coat} (μF cm-2)	CPE_b (μF cm-2)	χ^2 (×10-3)
Al coating								
in sterile ASW								
After 1 day	8.99	2110 ± 0.58	185.9 ± 0.9	-	106.5	231.4	-	0.932
After 2 days	11.01	1625 ± 0.76	351.9 ± 0.26	-	247.3	73.32	-	2.06
After 7 days	10.04	3167 ± 1 .01	297.1 ± 0.21	-	150	77.95	-	1.62
After 30 days	7.37	6057 ± 1.05	664 ± 0.72	-	202.7	74	-	1.19
in ASW with bacteria								
After 1 day	7.26	2479 ± 0.87	70.51 ± 0.03	-	163.8	291.9	-	2.34
After 2 days	5.75	1959 ± 0.95	73.02 ± 0.04	-	363.4	446	-	1.27
After 7 days	5.63	2796 ± 1.26	182.3 ± 0.35	-	124.8	121.1	-	0.536
After 30 days	10.55	15230 ± 1.68	6672 ± 0.55	11.09 ± 0.06	445.1	299.8	18.8	0.849

coatings is proposed, as already shown in Fig. 5b. For the coating samples incubated in the bacteria-containing ASW for 30 days, the model differs from the one describing the samples incubated for 7 days (Fig. 5b-2 vs b-1). For the samples incubated for 30 days, apart from the passive film and the double layer, a continuous dense biofilm readily formed on the surfaces of Al coatings. According to the proposed models, the calculated parameters relevant to the impedance results are also provided in Table 1. The circuit $R_{coat}Q_{coat}$ represents the processes blocking the coating surface and corresponds to high-frequency impedance. The higher frequency time constant is related to solution/coating interface, and the lower frequency time constant is related to solution/substrate interface. It is noted that the impedance value increased for the coating samples after 30 days incubation. This can be attributed to the protective film or stabilized pre-existing protective film easily produced on the metal surface [47]. The highly increased R_{ct} value implies a high corrosion resistance. For the coatings, a significant shift in R_{ct} with exposure time is observed. This shift is presumably due to the formation of the biofilm and stabilized pre-existing protective film, which is evidenced by the better corrosion resistance exhibited by the samples incubated in the ASW with bacteria than those incubated in the bacteria-free ASW. After 30 days, R_{ct} for the Al coatings in the bacteria-containing ASW reaches 15.23 kΩ cm^2, indicating that the bacteria opt to attach on the surface of the coatings, in turn forming biofilm. The biofilm acts as a protective layer in the corrosive environment. In the bacteria-free ASW, the corrosive liquid penetrates relatively easily through the coating.

Polarization curves were recorded after EIS testing (after 7 and 30 days of immersion) for all the samples (Fig. 6). Potentiodynamic polarization examination of the samples incubated in the ASW with/without the bacteria suggests consistent results with those suggested by the EIS analyses. The SS 316L samples immersed in the sterile solution showed a higher positive E_{ocp} and a lower corrosion current in the anodic branch (Fig. 6a), indicating that the bacteria activity reduces the corrosion resistance of the samples in inoculated solution. These results corroborate the other electrochemical data and the same explanation given above could be applied. Only a qualitative analysis of the polarization curves was made for the SS 316L samples because there is no reason to use the Butler-Volmer equation to estimate the anodic and cathodic Tafel coefficients. Therefore, all results obtained under the conditions used in this work indicate that the corrosion resistance of SS 316 L in presence of *Bacillus* sp. decreases significantly as compared to sterile medium. For the Al coatings immersed in the bacteria-containing ASW for 7 days, the cathodic current increases, while the anodic branch almost coincides with the anodic branch in the bacteria-free ASW. After 30 days exposure in the bacteria-containing ASW, corrosion potential of the coating shifts negatively, but corrosion current density drops (Fig. 6b). As expected from the EIS results, the corrosion current density I_{corr} for the Al coating in the bacteria-containing ASW is lower than that for the coating in the bacteria-free solution. In the bacteria-containing ASW, both the anodic and the cathodic curves shift to the left and the anodic and cathodic currents decrease after 30 days incubation. As discussed in previous section, the decreased I_{corr} of the coatings incubated in the solutions is probably attributed to formation of the bacteria-associated biofilm and possible oxide layer formed on their surfaces. These layers act as a barrier protecting the coatings from the penetration of aggressive solutions, giving rise to the enhanced corrosion resistance. Accumulation of the oxide/hydroxide film on electrode surface likely diminishes dissolution of Al. Presence of chloride easily triggers resolving of this film by the interaction between $Al(OH)_3$ film and Cl^- ions, which produced $AlCl_3$ after a sufficiently long time [48]. The formation of biofilm in the bacteria-containing ASW probably stabilizes the oxide layer and accordingly prevents failure of the film.

FESEM images of the coatings after the Tafel polarization testing show clearly the damaged oxide layer, accounting for the occurrence of pitting as observed previously. The electrochemical corrosion variables, namely corrosion potential, E_{corr}, corrosion current density, I_{corr}, anodic Tafel slope, b_a, and cathodic Tafel slope, b_c, are tabulated in Table 2. The extrapolation of anodic and cathodic Tafel lines reveals the corrosion current density and the corrosion potential, and it should start 50–100 mV away from E_{corr} [49]. The corrosion current density of the Al coatings in the bacteria-containing ASW after 30 days incubation is 1.019 μA/cm^2, much lower than that of the Al coatings incubated in sterile medium,

Table 2
Polarization parameters of the Al coatings incubated in the sterile ASW and the *Bacillus* sp.-containing ASW (corrosion current is expressed as means ± SD from three independent experiments).

Sample	E_{corr} (V vs SCE)	I_{corr} (μA/cm^2)	βc (mV/decade)	βa (mV/decade)
After 7 days				
Al coating in sterile ASW	−1.079	3.427 ± 0.121	−87.9	121.8
Al coating in *Bacillus* sp.-containing ASW	−1.055	4.352 ± 0.204	−110.4	133.5
After 30 days				
Al coating in sterile ASW	−0.898	2.048 ± 0.190	−91.85	101.8
Al coating in *Bacillus* sp.-containing ASW	−1.009	1.019 ± 0.242	−109.2	191.9

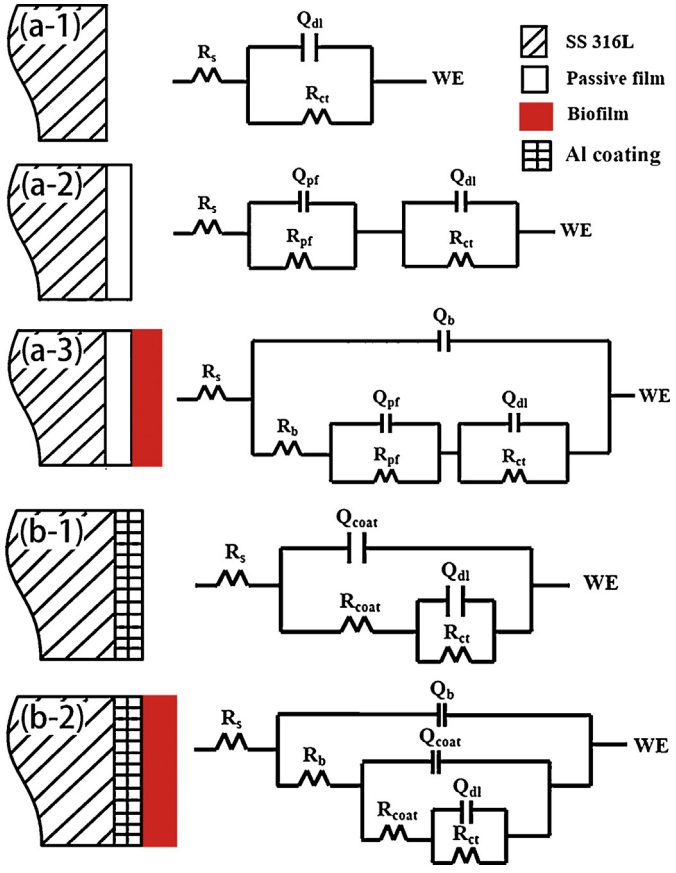

Fig. 5. Equivalent circuit models simulating the experimental impedance diagrams for the stainless steel coupons (a) and the Al coatings (b), (a-1) the model for the steel samples incubated for the first and second days in absence and presence of bacteria, (a-2) the model for the steel samples incubated for 7 and 30 days in bacteria-free ASW, and (a-3) the model for the steel samples incubated in bacteria-containing ASW for 7 and 30 days; (b-1) the model for the Al coatings soaked in bacteria-free ASW, and (b-2) the model for the Al coatings soaked in bacteria-containing ASW. R_s: solution resistance, Q_{pf}: capacitance of the passive film, R_{pf}: resistance of the passive film, Q_{dl}: capacitance of the double layer, R_{ct}: charge transfer resistance, Q_b: capacitance of the biofilm, R_b: resistance of the biofilm, Q_{coat}: capacitance of the coating, R_{coat}: resistance of the coating.

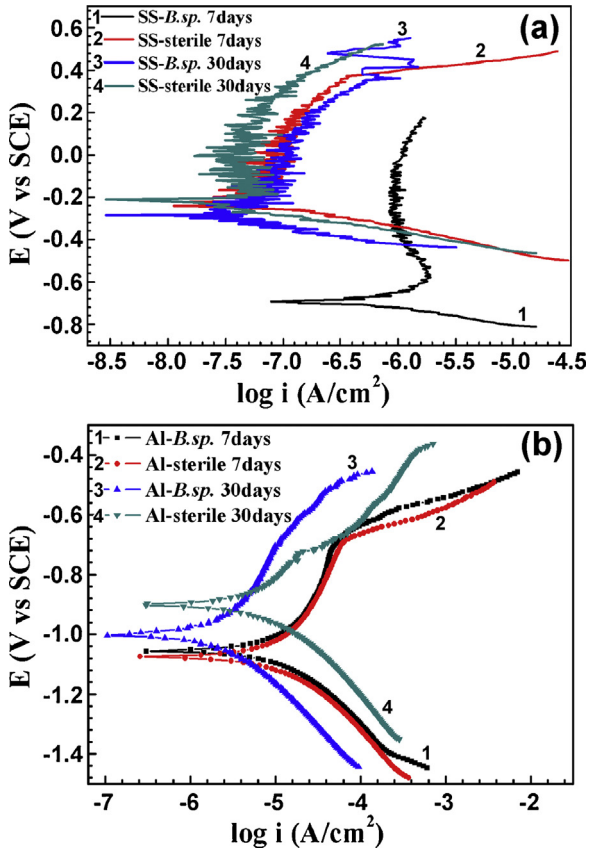

Fig. 6. Potentiodynamic polarization curves of the stainless steel plates (a) and the Al coatings (b) in the ASW with (-*B.*sp.) and without (-sterile) the bacteria after 7 days and 30 days of exposure. SS: SS 316L plates, Al: aluminum coatings.

2.048 μA/cm^2, suggesting better anti-corrosion performances of the coatings in inoculated media.

4. Conclusions

Attachment and colonization behaviors of marine bacterium *Bacillus* sp. on stainless steel and thermal sprayed aluminum coatings have been characterized. Surface roughness plays crucial roles in deciding adhesion of the bacteria on the surfaces, and rough surface facilitates attachment of the bacteria and subsequent formation of biofilm. Systematic investigation by using electrochemical testing approach has revealed distinctive effect of the biofilm on corrosion process of the steel and thealuminum coatings. Biofilm and the physicochemical characteristics of substratum materials play synergistic roles in deciding the corrosion of the materials. Presence of the biofilm continuously accelerates the corrosion of the steel in artificial seawater. However, the homogenous bacterial biofilm in early stage enhances the corrosion resistance of the aluminum coatings. Further growth of the biofilm is accompanied with pitting, giving rise to deteriorated corrosion of the coatings. The results shed some light on designing surface morphology and selection of materials for fabricating surface coatings for marine applications.

Acknowledgements

This research was supported by National Natural Science Foundation of China (grant 31271017, 41476064, and 51401232) and Project of Scientific Innovation Team of Ningbo (grant # 2015B11050).

Appendix A. Supplementary data

Supplementary data associated with this article can be found, in the online version, at http://dx.doi.org/10.1016/j.colsurfb.2016.05.075.

References

[1] P. Cristiani, G. Perboni, Bioelectrochemistry 97 (2014) 120.
[2] S.G. Gomez de Saravia, M.F.L. de Mele, H.A. Videla, Corrosion 46 (1990) 302.
[3] J.D. Gu, M. Roman, T. Esselman, R. Mitchell, Int. Biodeterior. Biodegradation 41 (1998) 25.
[4] Z. Lewandowskiy, W. Dickinsony, W. Leey, Water Sci. Technol. 36 (1997) 295.
[5] D.A. Jones, P.S. Amy, Corrosion 58 (2002) 638.
[6] B. Little, R. Ray, Corrosion 58 (2002) 424.
[7] D. Ornek, T.K. Wood, C.H. Hsu, Z. Sun, F. Mansfeld, Corrosion 58 (2002) 761.
[8] K.A. Zarasvand, V.R. Rai, Int. Biodeterior. Biodegradation 87 (2014) 66.
[9] V. Scotto, R.D. Cintio, G. Marcenaro, Corros. Sci. 25 (1985) 185.
[10] A.C. Dexter, D.J. Duquette, O.W. Siebert, H.A. Videla, Corrosion 47 (1991) 308.
[11] E. Juzeliunas, R. Ramanauskas, A. Lugauskas, K. Leinartas, M. Samulevicene, A. Sudavicius, Electrochim. Acta 51 (2006) 6085.
[12] M. Alnnasouri, C. Lemaitre, C. Gentric, C. Dagot, M. Pons, Biochem. Eng. J. 57 (2011) 38.
[13] K. Pedersen, Water Res. 24 (1990) 239.
[14] S.H. Flint, J.D. Brooks, P.J. Bremer, J. Food Eng. 43 (2000) 235.
[15] T. Lie, J. Periodont. Res. 12 (1977) 73.
[16] T. Lie, J. Periodont. Res. 13 (1978) 391.
[17] T. Lie, Acta Odontol. Scand. 37 (1979) 73.
[18] S.J. Yuan, S.O. Pehkonen, Colloids Surf. B 59 (2007) 87.
[19] X. Sheng, Y. Ting, S.O. Pehkonen, Corros. Sci. 49 (2007) 2159.
[20] H. Katayama, S. Kuroda, Corros. Sci. 76 (2013) 35.
[21] D. Chaliampalias, G. Vourlias, E. Pavlidou, G. Stergioudis, S. Skolianos, K. Chrissafis, Appl. Surf. Sci. 255 (2008) 3104.
[22] Y. Wang, Y.G. Zheng, W. Ke, W.H. Sun, W.L. Hou, X.C. Chang, J.Q. Wang, Corros. Sci. 53 (2011) 3177.
[23] J. Kawakita, S. Kuroda, T. Fukushima, T. Kodama, Corros. Sci. 45 (2003) 2819.
[24] V.R.S. Sa Brito, I.N. Bastos, H.R.M. Costa, Mater. Design 41 (2012) 282.
[25] H. Katayama, S. Kuroda, Corros. Sci 76 (2013) 35.
[26] M. Campo, M. Carboneras, M.D. López, B. Torres, P. Rodrigo, E. Otero, J. Rams, Surf. Coat. Technol. 203 (2009) 3224.
[27] X.D. He, X.M. Shi, Prog. Org. Coat. 65 (2009) 37.
[28] R.Z. Zand, K. Verbeken, A. Adriaens, Int. J. Electrochem. Sci. 7 (2012) 9592.
[29] F. Ahimou, M.J. Semmens, G. Haugstad, P.J. Novak, Appl. Environ. Microbiol. 73 (2007) 2905.
[30] T.M.P. Nguyen, X. Sheng, Y. Ting, S.O. Pehkonen, Ind. Eng. Chem. Res. 47 (2008) 4703.
[31] K. Kinzler, T. Gehrke, J. Telegdi, W. Sand, Hydrometallurgy 71 (2003) 83.
[32] W. Sand, Geothermics 32 (2003) 655.
[33] T. Rohwerder, T. Gehrke, K. Kinzler, W. Sand, Appl. Microbiol. Biotechnol. 63 (2003) 239.
[34] I.B. Beech, C.L.M. Coutinho, Biofilms in Medicine, Industry and Environmental Biotechnology-Characteristics, Analysis and Control, in: P. Lens, A.P. Moran, T. Mahony, P. Stoodly, V. O'Flaherty (Eds.), IWA Publishing, Alliance House, 2003, p. 115.
[35] G. Long, P. Zhu, Y. Shen, M. Tong, Environ. Sci. Technol. 43 (2009) 2308.
[36] Z. Filip, S. Hermann, Eur. J. Soil Biol. 37 (2001) 137.
[37] A. Kerr, M. Cowling, Philos. Mag. 83 (2003) 2779.
[38] B. Li, B.E. Logan, Colloids Surf. B 36 (2004) 81.
[39] I.B. Beech, J.R. Smith, A.A. Steele, I. Penegar, S.A. Campbell, Colloids Surf. B 23 (2002) 231.
[40] H.H. Fang, K.Y. Chan, L.C. Xu, J. Microbiol. Methods 40 (2000) 89.
[41] M. Itagaki, T. Suzuki, K. Watanabe, Corros. Sci. 40 (1998) 1255.
[42] E.J. Perez, R. Cabrera-Sierra, I. Gonzalez, F. Ramirez-Vives, Corros. Sci. 49 (2007) 3580.
[43] X. Shi, R. Avci, M. Geiser, Z. Lewandowski, Corros. Sci. 45 (2003) 2577.
[44] T. Shibata, T. Takeyama, Corrosion 33 (1977) 243.
[45] S. Bayoudh, A. Othmane, L. Ponsonnet, H.B. Ouada, Colloids Surf. A 318 (2008) 291.
[46] B. Szczygiel, M. Kolodziej, Electrochim. Acta 50 (2005) 4188.
[47] H.A. Videla, Rev. Metal. Madrid Vol. Extr. (2003) 256–264.
[48] S.S. Kale, V.S. Raja, A.K. Bakare, Corros. Sci. 75 (2013) 318.
[49] E. Poorqasemi, O. Abootalebi, M. Peikari, F. Haqdar, Corros. Sci. 51 (2009) 1043.